The EMBO Journal (2004) 23, 2963–2971 | © 2004 European Molecular Biology Organization | All Rights Reserved 0261-4189/04
www.embojournal.org

THE EMBO JOURNAL

Structure of the bifunctional and Golgi-associated formiminotransferase cyclodeaminase octamer

Yuxin Mao[1,4,5], Nand K Vyas[2,4], Meenakshi N Vyas[1], Dong-Hua Chen[2,3], Steven J Ludtke[2,3], Wah Chiu[2,3] and Florante A Quiocho[1,2,*]

[1]Howard Hughes Medical Institute, Baylor College of Medicine, Houston, TX, USA, [2]Verna and Marrs McLean Department of Biochemistry and Molecular Biology, Baylor College of Medicine, Houston, TX, USA and [3]National Center for Macromolecular Imaging, Baylor College of Medicine, Houston, TX, USA

Mammalian formiminotransferase cyclodeaminase (FTCD), a 0.5 million Dalton homo-octameric enzyme, plays important roles in coupling histidine catabolism with folate metabolism and integrating the Golgi complex with the vimentin intermediate filament cytoskeleton. It is also linked to two human diseases, autoimmune hepatitis and glutamate formiminotransferase deficiency. Determination of the FTCD structure by X-ray crystallography and electron cryomicroscopy revealed that the eight subunits, each composed of distinct FT and CD domains, are arranged like a square doughnut. A key finding indicates that coupling of three subunits governs the octamer-dependent sequential enzyme activities, including channeling of intermediate and conformational change. The structure further shed light on the molecular nature of two strong antigenic determinants of FTCD recognized by autoantibodies from patients with autoimmune hepatitis and on the binding of thin vimentin filaments to the FTCD octamer.

The EMBO Journal (2004) **23,** 2963–2971. doi:10.1038/sj.emboj.7600327; Published online 22 July 2004
Subject Categories: structural biology; proteins
Keywords: hepatitis autoantigen; intermediate channeling; protein assembly; structure; vimentin

Introduction

Formiminotransferase cyclodeaminase (FTCD) is present in every mammalian cell type either free in the cytosol or tightly bound to the Golgi complex, but is most highly abundant in the liver (Bashour and Bloom, 1998; Gao *et al*, 1998; Solans *et al*, 2000). The enzyme comprises of two (FT and CD) domains (Murley and MacKenzie, 1995). It catalyzes two key consecutive reactions that couple histidine degradation to folate metabolism (for review, see Shane and Stokstad, 1984). The FT activity transfers the formimino group from formimino-L-glutamic acid, a product of the histidine catabolism, to the N5 position of tetrahydrofolate (THF) to produce *N*5-formimino-THF and glutamate. The *N*5-formimino-THF is then channeled to the deaminase catalytic site where it undergoes cyclization to produce *N*5,*N*10-methenyl-THF and ammonia. *N*5,*N*10-methenyl-THF is an important precursor for the direct conversion of active coenzymes such as *N*5-formyl-THF and *N*10-formyl-THF and for the biosynthesis of several nucleotides, as well as other molecules, including *S*-adenosylmethionine and formylmethionine tRNA.

In addition to its metabolic function, FTCD is believed to play other cellular functions as a result of its tight association with the Golgi complex (Bashour and Bloom, 1998; Gao *et al*, 1998), although very little is known regarding the biochemical nature of this association. Recent studies have demonstrated that Golgi-associated FTCD binds to vimentin filaments *in vivo* and *in vitro*, and that its overexpression causes dramatic rearrangements of the vimentin IF cytoskeleton (Gao and Sztul, 2001). Further investigation also showed that direct interactions of the FTCD with vimentin filaments causes bundling of the filaments, which originates at the Golgi (Gao *et al*, 2002). Moreover, binding of vimentin filaments and regulation of filament assembly by FTCD require the intact octameric structure of FTCD but not its catalytic activity. No filament bundling is observed with isolated FT and CD domains (Gao *et al*, 2002). Taken together, these data support a role that, in addition to its enzymatic activity, FTCD acts as a structural–functional mediator between Golgi elements and the IF cytoskeleton.

FTCD is also associated with two human diseases. First, it is the specific autoantigen recognized by the anti-liver cytosol type 1 (LC1) autoantibodies present in patients with type 2 autoimmune hepatitis (AIH) (Lapierre *et al*, 1999), a disease that is lethal if left untreated (Johnson and McFarlane, 1993). Interestingly, two dominant linear antigenic determinants (^{428}NTPEEKD^{434} and ^{440}LQEGLRRA^{447}) in FTCD that interact with LC1 autoantibodies have been identified and further shown to exhibit sequence similarities with segments of antigenic virion proteins from human herpes virus type 6 (HHV-6) (Lapierre *et al*, 2003). This molecular mimicry between the FTCD autoantigen and viral antigens led to the suggestion that HHV-6 could be the trigger of type 2 AIH. Taken together, these features of AIH make FTCD an excellent paradigm for understanding the molecular basis of autoimmune diseases, such as systemic lupus erythematosus (SLE), which is also believed to be caused by Epstein–Barr virus by way of mimicry between its nuclear antigen EBNA and a ribonucleoprotein SLE autoantigen (Incaprera *et al*, 1998). Second, FTCD is also linked with FIGLU-URIA, a disorder associated with deficiency of glutamate formiminotransferase, which is the second most common inborn error of folate metabolism (Rosenblatt, 1995). Clinical manifestations of the deficiency range from mental and physical retardation to massive excretion of formiminoglutamate. Here we report the structure determination and functional analysis of the rat

*Corresponding author. Howard Hughes Medical Institute, Baylor College of Medicine, One Baylor Plaza, Houston, TX 77030, USA. Tel.: +1 713 798 6565; Fax: +1 713 798 8516;
E-mail: faq@bcm.tmc.edu
[4]These authors contributed equally to this work
[5]Present address: Department of Cell Biology, Yale University School of Medicine, New Haven, CT 06510, USA

Received: 10 May 2004; accepted: 21 June 2004; published online: 22 July 2004

FTCD by X-ray crystallography, electron cryomicroscopy (cryo-EM) and site-directed mutagenesis.

Results and discussion

Crystal structure, two-domain subunit and hinge-bending motion

The crystal structure, with four subunits in the asymmetric unit, was determined by multiple anomalous dispersion technique and refined to 3.4 Å resolution (Materials and methods and Table I). The structure of the 541-residue subunit consists of two distinct domains, the N-terminal FT and the C-terminal CD domains (Figure 1A), which are linked by an eight-residue segment (residues 327–334) (Figures 1A and 2). The FT domain is further made up of two subdomains, identified as N- and C-subdomains, which are bisected by a groove or a large cleft. As originally found for the structure of the isolated FT domain of porcine FTCD (Kohls *et al*, 2000), both subdomains show a similar α/β motif. In complete contrast, the CD domain folds into a long five-helix bundle. The relative orientation of both domains (Figure 1A) shows a subunit structure that is thin in one direction (40 Å) and thick in the two other directions (70 × 70 Å). The more globular FT domain has dimensions of about 60 × 45 × 40 Å. In contrast, the long helix bundle structure of the CD domain is reflected in its dimensions of 70 × 30 × 25 Å. As shown in Figure 1A, there is only one major interdomain contact, which buries a total of ∼465 Å^2 of surface area. It is also notable that the FT groove opening is directed away from the CD domain.

An overlap of the FT domain in the ligand-free subunit (Figure 1B) with the crystal structure of only the isolated FT domain with a bound product analog folinic acid (Kohls *et al*, 2000) demonstrates for the first time that the domain undergoes a large conformational change by way of a hinge-bending motion of about 30° between the two subdomains (Figure 1B). This motion modulates access to and from the active site groove, including intermediate channeling, and enables both subdomains, following groove closure, to engage in binding and sequestering the substrates and in the ensuing FT catalytic activity.

D_4 or square doughnut FTCD quaternary structure

The quaternary structure of FTCD is essential for the expression of the two sequential catalytic activities, including

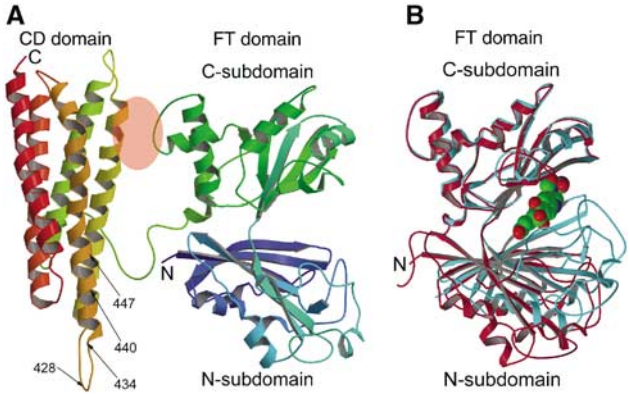

Figure 1 Subunit structure of FTCD. **(A)** The two-domain (FT and CD) subunit structure of the ligand-free FTCD. Backbone trace color ramped from the N-terminal end (N) to the C-terminal end (C). In this orientation, the lengths of the top and bottom and the two sides are roughly 70 Å and the thickness is about 40 Å. The areas of the FT C-subdomain and CD domain shaded in pink oval are involved in the only interdomain interaction within the subunit, which is mainly between the segment of residues 290–295 of the FT C-subdomain and residues 392–399 of the CD domain (refer also Figure 2). The arrows demarcate the locations of the two major linear antigenic determinants (^{428}NTPEEKD^{434} and ^{440}LQEGLRRA^{447}) of human FTCD autoantigen (Lapierre *et al*, 2003), which differ by only one residue from the same segments in rat FTCD (see text). **(B)** Superpositioning of the C-subdomain of the FT domain in the subunit (red) structure (panel A) with that in the structure of the same domain in isolation (aqua marine) with the product analog, folinic acid (CPK model), bound in the groove (Kohls *et al*, 2000). The orientation of the FT domain is identical to that shown in panel A. The groove in the ligand-free structure of the intact subunit is wide open, whereas that in the ligand-bound structure of the isolated FT domain is completely closed.

Table I Data collection, phasing statistics and refinement

	MAD phasing data			Refinement data
	SeMet λ1 (peak)	SeMet λ2 (inflection)	SeMet λ3 (remote)	SeMet λ1 (peak)
Data collection and phasing				
Wavelength (Å)	0.9791	0.9793	0.9716	0.9791
Resolution (Å)	50–4.0	50–4.0	50–4.0	50–3.4
Total observations	178 995	177 050	168 800	249 272
Unique reflections	42 757	41 005	40 917	67 690
Completeness (%)[a]	94.9 (91.2)	87.0 (78.5)	86.4 (75.8)	92.1 (86.7)
$\langle I\rangle/\langle\sigma\rangle$[a]	9.8 (4.2)	8.9 (3.2)	6.7 (2.4)	6.0 (1.9)
R_{sym}[a,b]	0.094 (0.158)	0.097 (0.174)	0.112 (0.206)	0.113 (0.249)
Phasing power[c]	2.1	1.5	—	—
Refinement				
Resolution (Å)		10–3.4		
R_{crys}/R_{free} (%)[d]		24.6/28.8		
R.m.s. bond length (Å)		0.009		
R.m.s. bond angle (deg)		1.5		

[a]Values in parentheses are for the highest resolution shell.
[b]$R_{sym} = \sum_h\sum_i|I_I(h) - <I(h)>|/\sum_h\sum_i I_I(h)$.
[c]Phasing power is the r.m.s. value of F_h divided by the r.m.s. lack-of-closure error.
[d]$R_{crys} = \sum(|F_{obs}| - k|F_{cal}|)/\sum|F_{obs}|$. R_{free} was calculated for 5% of reflections randomly excluded from the refinement.

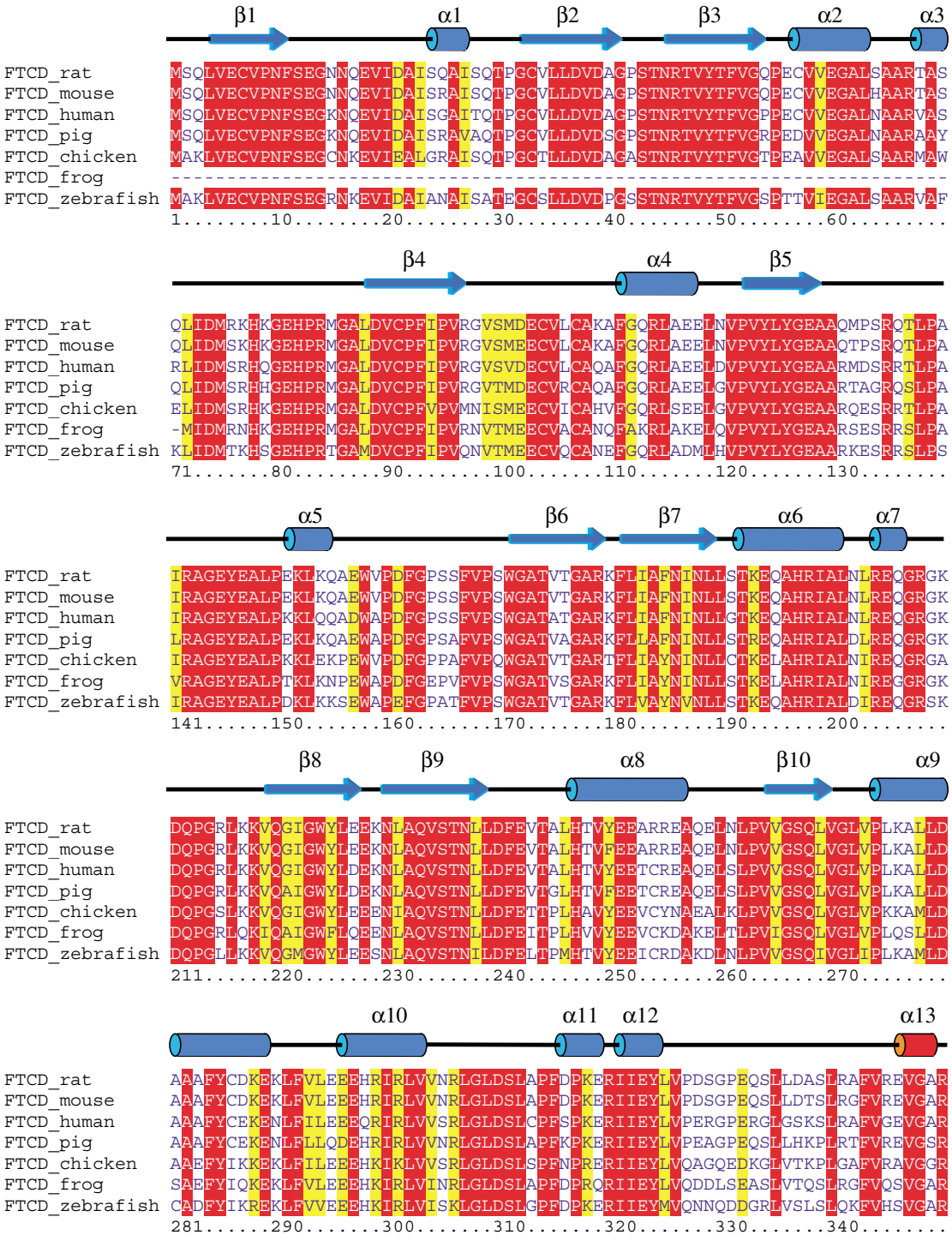

Figure 2 Secondary structure of rat FTCD monomer and multiple alignment of FTCD amino-acid sequences. The secondary structure elements of the FTCD crystal structure are drawn above the alignment with the rat protein sequence as reference, and those that are colored blue and red belong to the FT and CD domains, respectively. The alignment was obtained using the Clustal W program and colored by the Boxshade program. Only invariant and highly conserved residues are highlighted in red and yellow backgrounds, respectively.

channeling of intermediate (Findlay and MacKenzie, 1988), and for its interaction with the vimentin intermediate filament cytoskeleton (Gao *et al*, 2002). Examination of the molecular packing arrangement within the crystal lattice revealed a compact octamer with four of the pair of subunits 1 and 2 in the asymmetric unit structure packed tightly around the crystallographic four-fold rotational axis (Figure 3A). This organization creates two four-subunit layers: those of subunit 1 are in an anticlockwise head-to-tail arrangement and those of subunit 2 in a clockwise arrangement (Figure 3A and B). The octamer exhibits a 422 or D_4 point group symmetry and an overall shape of a square doughnut with outside and inside widths of 140 and 35 Å, respectively, and a height of 110 Å.

To further ascertain the D_4 model, we performed a cryo-EM 3D reconstruction of randomly oriented single particles

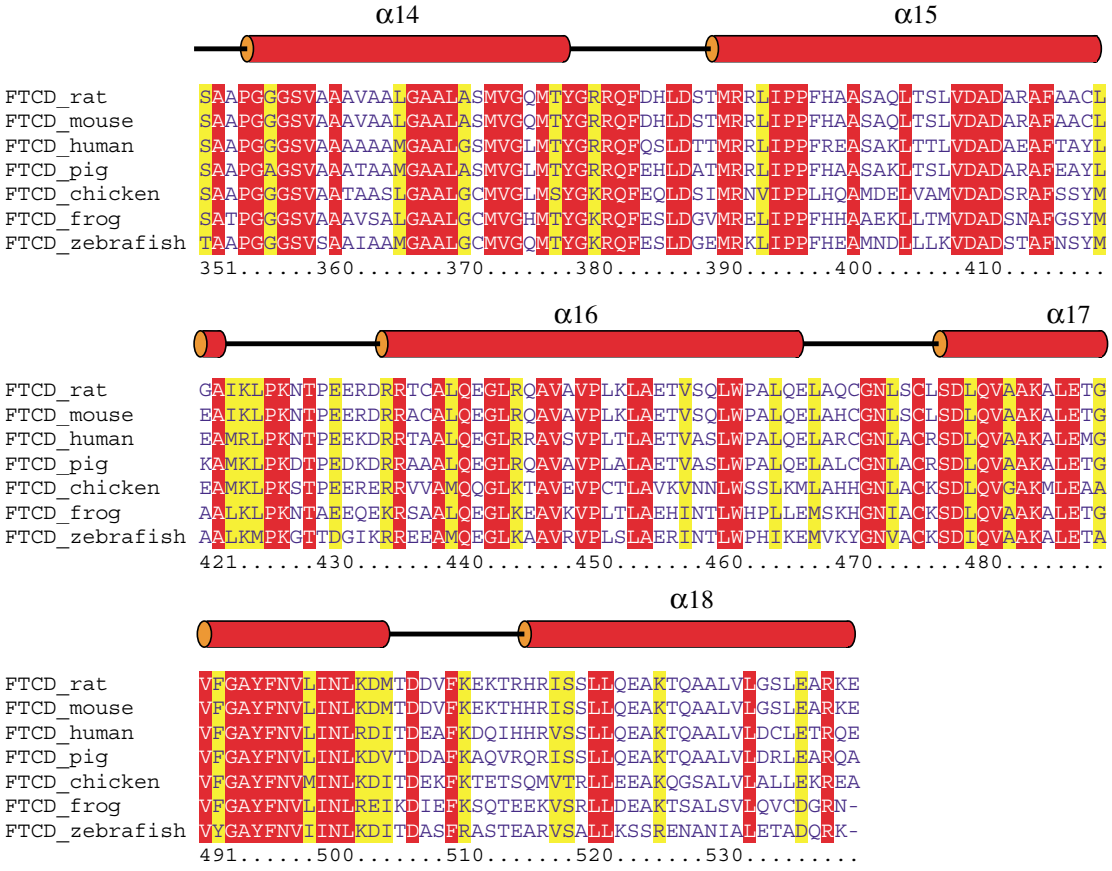

Figure 2 Continued

(Figure 4). The mass density (Figure 5A) clearly showed a square doughnut protein particle with undulating surface on both ends owing to alternating dome-like features, those from the sides jutting out farther than those from the corners. As shown in Figures 5B and C, the D_4 model fits well to the reconstruction density, thus establishing the FTCD quaternary structure, which is named D_4 or square doughnut octamer.

A totally different model of FTCD octamer, named 'planar ring model', was proposed 28 years ago based on visual analysis of EM images of negatively stained FTCD samples (Beaudet and Mackenzie, 1976). The outside and inside diameters of the planar ring are 116 and 53 Å, respectively. The analysis also indicated a diameter of 32 Å for a subunit, which is no larger than any of the dimensions of the FT domain (Figure 1A).

Major intersubunit interactions in the FTCD octamer

The elaborate organization and interactions of the eight identical subunits in the D_4 octamer shed light on the stability and catalytic activities of the octamer. Each subunit is engaged mainly in two isologous and one heterologous interactions that stabilize the octamer. The two isologous interactions, as shown for example for subunit 1 in Figure 6A (see also Figure 3A and B), are formed by the local two-fold related association of the FT and CD domains with the FT domain of subunit 2‴ and the CD domain of subunit 2, respectively. The FT–FT pair, which is mediated by the interaction between C-subdomains, occupies mainly the sides of the square doughnut-shaped octamer, whereas the CD–CD pair of helix bundles occupies the corners. The alternating FT–FT and CD–CD pairs (Figures 3A and 6A) constitute the tall and short domes, respectively, that are seen in the cryo-EM density (Figure 5). The observation that the isologous interaction between the CD domains buries ~3800 Å^2 of surface area (or ~1900 Å^2 per domain) using a 1.4 Å probe radius and that between the FT C-subdomains occludes ~1900 Å^2 of surface area (or ~950 Å^2 per subdomain) indicates considerable stability of the two interactions. This is consistent with the finding that each domain in isolation forms monofunctional homodimers (Murley and MacKenzie, 1995). Our quaternary structure analysis further uncovered a less extensive but apparently functionally important (discussed below) heterologous interaction between the FT C-subdomain (e.g., of subunit 1) and the CD domain (e.g., of subunit 2‴) (Figure 6A and B), which accounts for ~690 Å^2 of total buried surface. The interactions associated with the quaternary structures, especially the two different isologous interactions, have two significant structural and functional consequences. First, since the contact between the CD domains is more extensive than that between the FT C-subdomains, it provides greater stability to the entire octamer structure. This finding is consistent with denaturation studies, which indicated two types of isologous subunit–subunit interactions in FTCD, although their relative stability was uncertain (Murley and MacKenzie, 1997). The determination of the FTCD octamer structure has now provided an atomic basis for the relative stability and nature of two different

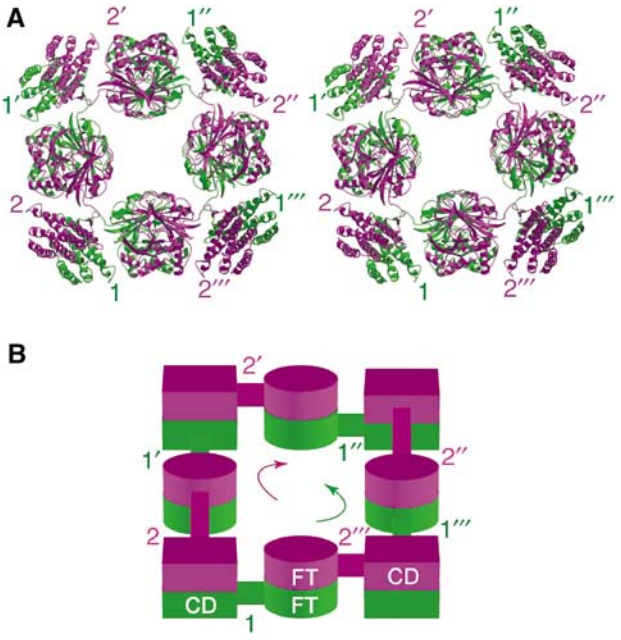

Figure 3 D_4 quaternary structure of FTCD. (**A**) Stereo view of the compact D_4 octamer looking down the crystallographic four-fold rotation axis. The octamer generated by crystal packing consideration has four of the pair of subunits 1 (green) and 2 (purple) in the asymmetric unit structure packed tightly around the crystallographic four-fold rotational axis. The four pairs of subunits 1 and 2 that make the octamer are identified by unprimed and primed numbers. Local two-fold rotation axes every 45° bisect the octamer in the horizontal plane. In this view, the four purple subunits (numbered 2s) of the upper layer are in a clockwise head-to-tail arrangement and the four green subunits (numbered 1s) of the lower layer are in an anticlockwise arrangement. An equivalent octamer (not shown) has four pairs of subunits 3 and 4 in the asymmetric unit packed around another four-fold axis. (**B**) Schematic diagram of the lower (green) and upper (purple) four-subunit layers of subunits as shown in panel A. The arrows indicate the directions of the head-to-tail arrangements of the four subunits in each separate layer.

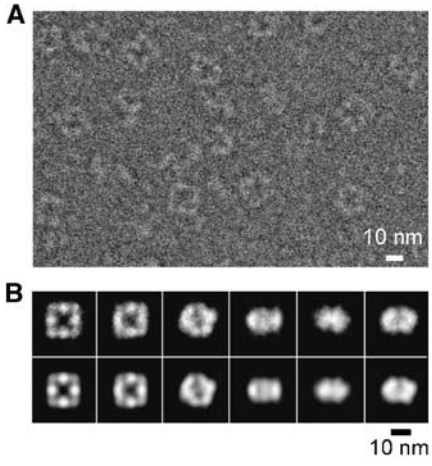

Figure 4 Cryo-EM analysis of FTCD at 20 Å resolution. (**A**) An area of a typical image (× 50 000 magnification) of ice-embedded FTCD recorded in JEOL 2010F electron cryomicroscope at a dose of 18.6 electrons/Å^2 and 4.1 μm defocus (see Materials and methods). (**B**) Examples of characteristic views used to reconstruct the three-dimensional structure (top row) and corresponding reprojections from the three-dimensional reconstruction (bottom row). Some of the characteristic views, especially the left most pair, clearly show the characteristic four-fold symmetry and square doughnut shape of the octamer.

isologous interactions. Second, since the N-subdomain of the ligand-free FT domain is essentially free from any interaction in the octamer (Figures 3A and 6A), while the C-subdomain is clamped not only by intersubunit interactions with an FT C-subdomain and a CD domain (Figure 6A and B) but also by an intrasubunit interaction with its CD domain (Figure 1A), the N-subdomain is almost certainly the one that moves in the hinge-bending motion described above.

Cyclodeaminase active site

The location of transferase active site is known, which is in a groove between the two FT subdomains (Figure 1B), but that of the deaminase catalytic site is yet to be pinpointed. The CD domain by itself does not have any major groove or cleft (Figure 1A). However, the deep pocket in both ends of the local two-fold related CD–CD pair of helix bundles (Figure 6) in the FTCD octamer became the prime candidate for the deaminase active site. The pocket is made up of about 36 solvent-exposed residues with very high conservation (86% invariant and 8% conserved) in mammalian FTCDs. To prove that the pocket is the CD active site, we carried out site-directed mutagenesis of some of the residues that are invariant and lining the pocket (see Materials and methods). Mutations D412A or D412N completely abolished deaminase activity, while M373A, N501A and D479V reduced the activity to 70, 20 and 10%, respectively, of wild-type activity. Residues D412 and D479 were particularly chosen because they are almost in the bottom of the pocket, a region of the pocket that the pteridin ring of the substrate might occupy. It has been observed that negative charged surface is near the binding site of the tetrahydropteroyl group of the folinic acid bound to the isolated FT domain crystal structure (Kohls *et al*, 2000). Mutations of residues outside the pocket (e.g., L370, L444 and D504) to Ala residues have no effect on activity. The results indicate that the cyclodeaminase active site is located in a deep pocket at the ends of the long CD–CD pair of bundle of helices.

Intermediate channeling

Intermediate channeling is an important process in multi-catalytic enzymes for the direct transfer of metabolic intermediates from one catalytic site to another without prior equilibration with the bulk solvent (for review, see Huang *et al*, 2001). The elucidation of the quaternary structure provides new understanding of the process in FTCD. The best possible route for channeling the 5-formimino-THF intermediate, which is theoretically repeated eight times in the D_4 octamer, is from the FT active site groove of one subunit (e.g., subunit 1) to the CD active site pocket formed between the CD domains of two other subunits (e.g., 2‴ and 1‴) (Figure 6A and B). This pathway is the most direct and the shortest distance (∼35 Å) between the two different catalytic sites as measured between the positions of the N5 atom of the folinic acid bound in the FT active site and the α-carbon atom of Asp 412 in the CD active site pocket. Moreover, in this pathway, the opening of the FT site groove is directed toward the CD active site pocket. The partially enclosed environment of the FT active site groove and the CD active site deep pocket, combined with the presence of two helices (α15 and α16, see Figure 2) and connecting loop of subunit 1‴ CD domain towering above the deaminase active

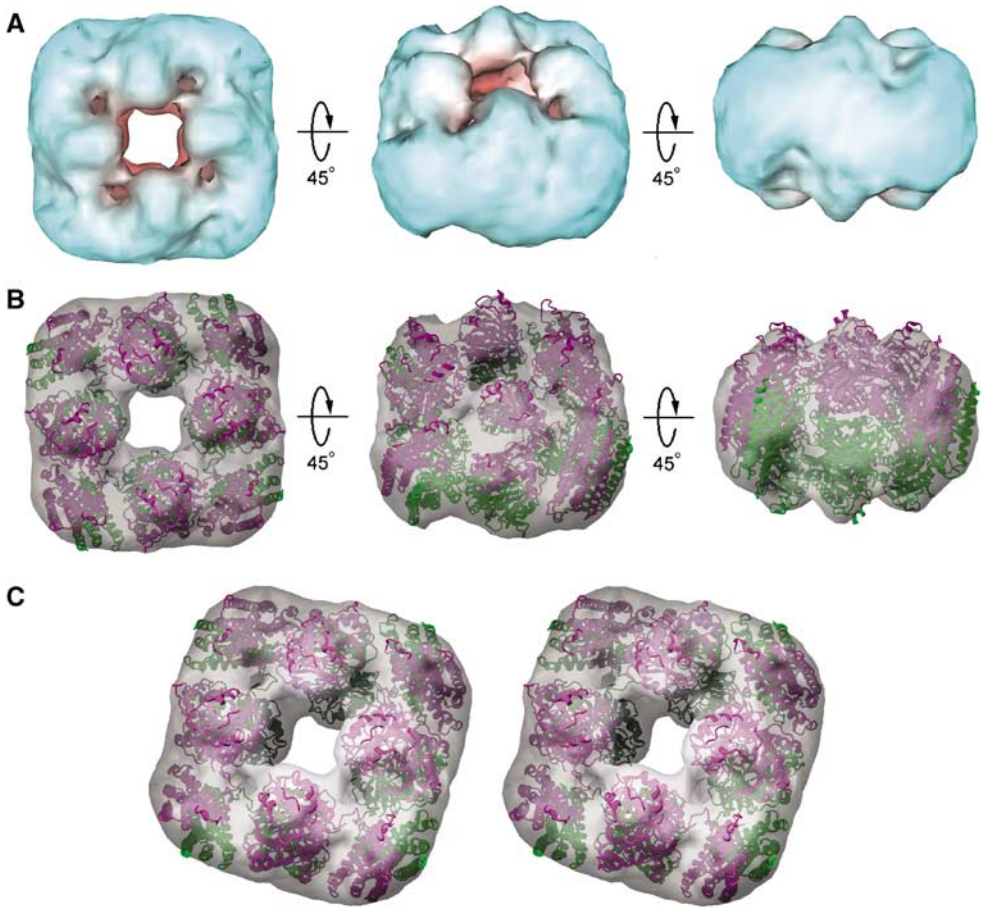

Figure 5 Cryo-EM reconstruction density and fit of the D_4 octamer. (**A**) Three views of the reconstruction density of FTCD contoured at 1.4σ. (**B**) Identical to panel A but with the density in semitransparent gray surface and the D_4 octamer (Figure 3A) fitted. The final crosscorrelation coefficient between the fitted D_4 model and the cryo-EM map is 0.82. (**C**) A tilted stereo view of the fit of the D_4 octamer to the cryo-EM density.

site (Figure 6A), could restrain the intermediate from dissociating into the bulk solution.

Our proposed new channeling mechanism could also satisfactorily take into account the finding that naturally occurring γ-linked polyglutamylated *N*5-formimino-THF is transferred directly between the two sites, with optimal efficiency for the pentaglutamate chain (MacKenzie and Baugh, 1980). This finding led to the proposition that the polyglutamate tail acts as a tether or a 'swinging arm' for the direct transfer of the pteroyl ring between active sites. Modeling of the pentaglutamate tail added on the folinic acid bound in the FT 'open' groove indicates that one or two terminal glutamates are within salt linking distance to some of the exposed mostly invariant basic residues that are concentrated at the interface of the heterologous interaction between the FT C-subdomain of one subunit and the CD domain of another subunit and are located nearly equidistant (∼25 Å) to the pteridin ring bound in the FT active site groove and the CD active site pocket (Figure 6B). The polyglutamate tail, anchored by the salt links, could then function as a swinging arm to shuttle the pteroyl ring of the intermediate from the FT groove to the CD active site pocket. Moreover, since the FT C-subdomain is closer to the positive center and firmly held in place, it could serve as the initial binding site of the polyglutamated THF substrate as well as the platform from which intermediate translocation originates. The entire channeling mechanism, together with the conformational change associated with the FT domain, is incorporated in the schematic representation of the major steps in the catalytic functions of FTCD (Figure 6C). The coupling of three subunits, by way of two isologous and one heterologous interactions, is the first concrete structural proof of the requirement of the quaternary structure of FTCD for catalytic functions, including intermediate channeling. Totally different models of intermediate channeling, assuming that the process occurs from the FT domain to the CD domain of only one subunit, and of polyglutamate tail binding with a different set of positive charge residues have been proposed (Kohls *et al*, 2000). Neither of these proposals takes into account the requirement of the quaternary structure.

Binding of FTCD to vimentin

Bundling of individual vimentin filaments, each with a diameter of about 10 nm, requires the intact FTCD octamer and binding of a maximum of four filaments to an FTCD octamer molecule (Gao *et al*, 2002). In the light of our FTCD D_4 quaternary structure, binding of individual filaments to four-fold related external surface sites that extend across the two four-subunit layers (Figure 3) satisfies the requirement. Moreover, given the octamer side of ∼14 nm width, binding of the filament of ∼10 nm diameter will be limited to no more than four sites (or one per side) of the FTCD square doughnut octamer. To further satisfy the requirement for an intact FTCD

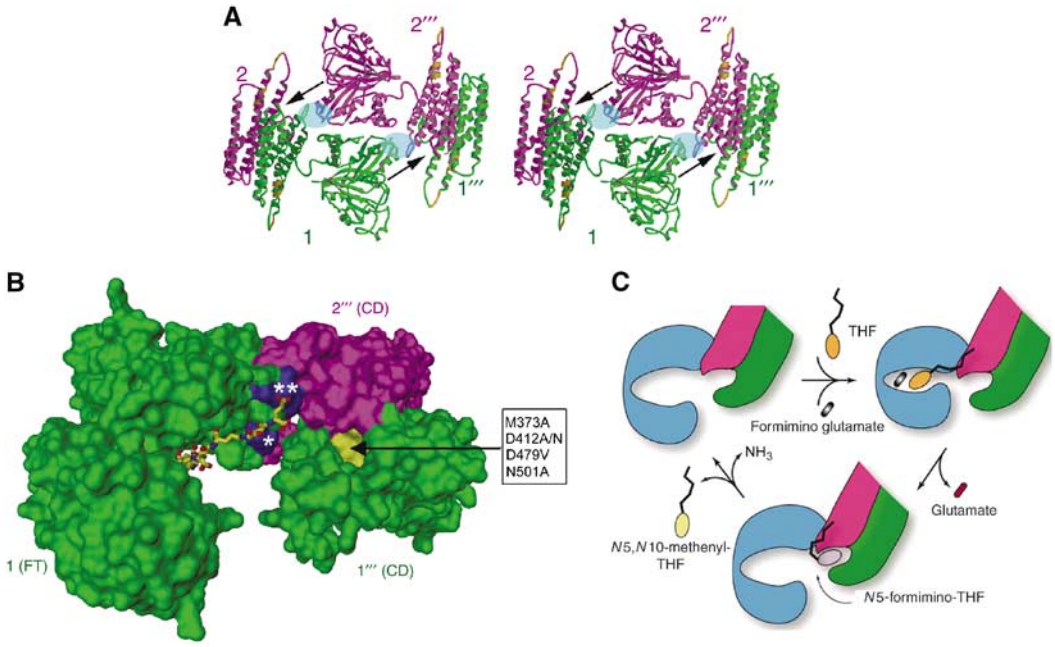

Figure 6 Subunit organization for enzyme activities and intermediate channeling. **(A)** Stereo view of one side of the D_4 octamer. The width of the side is about 140 Å or 14 nm. This view is orthogonal to that shown in Figure 3A. The side is occupied mainly by the isologous stack of two FT domains (e.g., between subunits 1 (green) and 2‴ (purple)). The FT–FT stack is flanked on both sides by isologous pairs of CD domain helix bundles of subunits 1 and 2 and subunits 2‴ and 1‴, which occupy the corners. Each of the arrows indicates the best possible route for channeling the *N*5-formimino-THF intermediate from the FT catalytic site groove in subunit 1 or 2‴ to the deaminase catalytic site pocket near the end of a pair of CD domains between subunits 2‴ and 1‴ or subunits 1 and 2, respectively. The deep pocket (see also panel B) at each end of the CD–CD pair is the only one found by the POCKET program (see Materials and methods). The local two-fold related areas shaded in blue oval represent regions involved in heterologous interactions, between the FT domain from one subunit and CD domain from another subunit. This interaction is mainly between the N-terminal end (residues 192–198) of helix α6 in the FT C-subdomain and the loop (residues 379–389) connecting helices α14 and α15 in the CD domain (see also Figure 2). The two nearly contiguous segments in the CD domain (gold) represent the equivalent two immunodominant linear epitopes recognized by LC1 autoantibodies (see text and Figure 1A). (**B**) Geometrical relationship between the FT domain active site groove, the CD active site pocket (yellow surface) and two adjacent patches (blue surface) of positive charge residues. This figure of molecular surface shows only the FT domain from subunit 1 and the two CD domains from subunits 2‴ and 1‴. The residues in the box (D479 and M373 from subunit 1‴ and D412 and N501 from subunit 2‴) are those in the CD pocket (directed by the arrow) that when mutated resulted in diminution of CD activity (see text and Materials and methods). The FT active site groove is in the open form with the pteroyl moiety of the folinic acid (stick model) bound in the C-subdomain as shown Figure 1B. The ligand has four additional γ-linked glutamates coupled to the glutamate of folinic acid to generate a five-residue polyglutamate tail. Modeling of the polyglutamate tail indicates potential salt links of the two terminal glutamates with highly conserved basic residues (Figure 2), including R/K 193, which lies in the patch (marked with a single asterisk) of subunit 1 FT C-subdomain, and R381 and R382, which lie in the patch (double asterisks) of subunit 2‴ CD domain. Arg residues (especially doublets such as arginines 381 and 382 in FTCD) have been implicated in the binding of polyglutamylated substrates to folate-dependent enzymes (Finer-Moore *et al*, 1994; Murley and MacKenzie, 1995). Indeed, we found that mutagenic replacement of Arg 382 to an Ala residue no longer allows FTCD to bind to the polyglutamate affinity column, which is very effective in the purification of the native protein (see Materials and methods). (**C**) Schematic diagram of the major steps of the dual enzyme activities of FTCD in the D_4 quaternary structure. The FT domain is colored blue to emphasize the involvement of three domains (including two CD domains truncated to show only one active site) from three subunits. Starting with the ligand-free FTCD (upper left), the substrates bind in the open form of the FT domain, with the THF (ring structures in orange) initially binding in the C-subdomain and thereby allowing the polyglutamate tail to form salt links with basic residues concentrated at the interface between the FT C-subdomain and CD domain (see panel B). The groove closes (upper right) by movement of the FT N-subdomain toward the C-subdomain, triggering transferase catalysis. The groove then opens (bottom model), thereby releasing the product glutamate and allowing the pteroyl ring (gray) of the *N*5-formimino-THF intermediate to be shuttled to the CD active site pocket by the swinging motion of the anchored polyglutamate tail for CD catalysis. In the final step, the two products (*N*5,*N*10-methenyl-THF (yellow pteridin ring) and ammonia) of the deaminase catalysis are released, and the starting open enzyme form is regenerated.

octamer, each of the four-fold related sites could include the surface area between FT–FT and CD–CD pairs, where the FT and CD domains are from one subunit (e.g., labeled 1s) and two different subunits (e.g., labeled 2s) (Figure 3).

Two major linear epitopes of the FTCD autoantigen for hepatitis autoantibody recognition

The sequences of two major linear antigenic determinants (^{428}NTPEEKD^{434} and ^{440}LQEGLRRA^{447}) of human FTCD autoantigen recognized by LC1 autoantibodies (Lapierre *et al*, 2003) differ by only one residue from the same segments in the aligned rat FTCD: Lys 433 and Arg 446 in human are respectively Arg and Gln in rat (Figure 2). Moreover, the sequences of rat and human FTCDs are 86% identical and 91% similar (Figure 2). Therefore, our structure provides an initial plausible view of the conformations and locations of these two epitopes, which are shown in Figure 1A. The peptide segment representing the first epitope lies in a more exposed and mobile loop, whereas the second epitope occurs near the N-terminus of a less flexible and mobile long amphiphatic helix (α16; Figures 1A and 2). It is further notable that the two nearly contiguous epitopes, which are coincidentally situated above the opening of the CD active site pocket (Figure 6A), are unobstructed in the D_4/square doughnut octamer (Figures 3A and 6A) and thus can be recognized by the autoantibodies.

Conclusion

New insights into the diverse functions and complex quaternary structure of FTCD have emerged from our combined X-ray crystallographic and electron cryomicroscopic investigations. These investigations reveal a subunit structure comprised of two domains with distinct motifs, a two-layer compact octamer structure resembling a square doughnut, two isologous and one heterologous interactions for octamer stability, and a three-domain cluster (one FT and two CD domains) from three subunits required for the dual enzyme activities and intermediate channeling. The crystal structure further demonstrated a hinge-bending motion between the two lobes of the FT domain and the different conformations (segments of a loop and a helix) and high accessibility of the two immunodominant linear epitopes of the FTCD autoantigen. It also takes into account the binding of no more than four thin vimentin filaments for filament crosslinking and bundling. Further biochemical and structural studies based on the tertiary structure are required to further deepen our understanding of the multiple functions of FTCD, including its association with the vimentin intermediate filament and/or the Golgi complex.

Materials and methods

Expression, purification and crystallization of FTCD

PET-21(b) plasmids containing the rat FTCD gene, kindly provided by Dr E Sztul (University of Alabama, Birmingham), were transformed into *Escherichia coli* BL21 cells. Cells were grown at 37°C to an OD_{600} of about 1.0. The temperature was then lowered to 16°C, and the cells were induced with 0.1 mM IPTG for 4 h. The cells were harvested and frozen at −70°C for later use.

Frozen cells from 3 l culture were thawed by adding 90 ml sonication solution of 1 mM EDTA, 1 mM PMSF, 15 mM β-ME and 100 mM K_3PO_4 (pH 7.4). Sonication was performed for 2 min four times, and the cell lysate was clarified by centrifugation at 22 000 rpm for 30 min. The supernatant (~90 ml) was pooled and supplemented with 2 ml of 1 M MOPS (pH 7.3) and 20 ml glycerol. Ammonium sulfate was gradually added to 40% saturation while stirring at 4°C. The mixture was then centrifuged at 22 000 rpm for 30 min. The pellet was resuspended in 50 ml of dialysis buffer (1 mM EDTA, 0.2 mM PMSF, 1 mM DTT, 1% glycerol, 20 mM K_3PO_4, pH 7.4) and dialyzed overnight with two changes of the dialysis buffer. The dialyzed solution was clarified by centrifugation at 22 000 rpm for 30 min and then mixed with 3 ml of polyglutamic acid linked to agarose beads and incubated for 3 h. The mixture was packed in a 5 ml disposable column and washed thoroughly with dialysis buffer. The bound FTCD protein was eluted with the elution buffer (dialysis buffer plus 1 M NaCl). The eluted protein is >90% pure. To remove minor contaminants, the protein was subjected to a gel filtration chromatography (Superdex 200) using the dialysis buffer as the eluting buffer. The FTCD protein, which eluted at the expected 0.5 million Dalton mass, was pooled and concentrated to 5 mg/ml for crystallization.

Initial condition for crystallization was screened against Wizard I and II formulations (Emerald BioStructure) using hanging drop vapor diffusion method. Crystals were eventually obtained from a 1:1 mixture of protein stock and reservoir solution containing 0.1 M Na_2SO_4, 15% (v/v) PEG 600 and 0.1 M HEPES (pH 7.6). Pyramid-shaped crystals usually appeared after a couple of days. For the crystallization of the selenomethionine variant of the protein, 10% glycerol, which stabilizes the protein and improves the quality of crystals, was added to the well solution before mixing with the protein stock.

X-ray structure determination

Before data collection, the crystals were mounted onto a CryoLoop loop, swished in the well solution, which contained 30% (v/v) PEG 600, and flash frozen in a nitrogen gas stream cooled at −150°C. X-ray data were collected at APS SBC 19ID beamline. Of about 100 crystals of the selenomethionine variant of FTCD that were screened for diffraction, only one gave diffraction data sufficient to solve by multiple anomalous dispersion technique and refine the structure (Table I). Three wavelength data were collected from this crystal with 0.5° per frame for a total of 480 frames. The three wavelength data were processed and scaled using HKL2000 program and SCALEPACK (Otwinowski and Minor, 1997). The crystal belongs to space group P4 with unit cell dimensions of $a=b=134.85$ Å and $c=156.37$ Å and four subunits in the asymmetric unit for a total of 32 selenium atoms. FTCD has always been shown (MacKenzie, 1980; Bashour and Bloom, 1998; Gao *et al*, 1998; Solans *et al*, 2000) to be composed of eight identical subunits with a total mass of about 0.5 million Dalton. Dynamic light scattering measurements of several protein preparations used in our crystallizations are consistent with the data.

The structure was determined by multiple anomalous dispersion method at 4 Å using SHAKE AND BAKE (Weeks *et al*, 1995). The top 16 heavy atom sites found were refined by SHARP (La Fortelle and Bricogne, 1997). After each round of refinement, additional selenium sites were verified by the FINDNCS program (Lu, 1999) in the CCP4 Package (Collaborative Computational Project No. 4, 1994). Only the sites that were related by NCS two-fold were kept for further rounds of refinement. After several rounds of heavy atom refinement, all 32 selenium sites were located. The initial MAD phases with a mean figure of merit of 0.41 at 4.0 Å resolution were improved considerably by solvent flattening and NCS averaging in CNS (Brünger *et al*, 1998). It was clear at this juncture that the subunit structure is composed of two totally different domains. The structure of the FT domain was first obtained by fitting each subdomain of the crystal structure of the isolated FT domain (Kohls *et al*, 2000). The *de novo* trace of the CD domain was built using O (Jones *et al*, 1991). The protein coordinates were refined initially with CNS at 3.7 Å using experimental phases and strict NCS followed by cycles of manual rebuilding using phase combined maps. The structure was ultimately refined against the 3.4 Å refinement data (Table I) by simulated annealing, conjugate gradient minimization, isotropic *B*-factor refinement and tight NCS restrain.

Cryo-EM structure determination

A droplet of FTCD in 1 mM DTT, 1 mM folinic acid and 20 mM phosphate buffer (pH 7.4) was applied to a quantifoil grid (R2/2, Quantifoil Micro Tools GmbH, Jena, Germany) and quickly frozen to liquid nitrogen temperature using the established procedure (Dubochet, 1988) and a fully automated vitrification device called Vitrobot (FEI Company) for plunge-freezing. Images were taken as focal pairs at ×50 000 magnification in a JEOL2010F electron cryomicroscope operated at 200 kV and specimen temperature −178°C with a dosage of about 18 electrons/$Å^2$ for each micrograph and recorded on Kodak SO-163 films. Micrographs (e.g., Figure 4) were digitized on a Nikon super coolscan 8000 scanner (Nikon Inc.) using a pixel size equivalent to 5.08 Å on the specimen. Three-dimensional maps were reconstructed at about 20 Å resolution using a total of 3227 digitized particle images using standard techniques in EMAN software (Ludtke *et al*, 2001) and were visualized by using the Explorer software package (NAG Inc., Downer's Grove, IL) with custom-designed modules. Fitting of octamer models derived from crystal packing consideration with the cryo-EM reconstruction density and calculating crosscorrelation coefficient of the fit were performed using *Foldhunter* (Jiang *et al*, 2001).

CD active site pocket, site-directed mutagenesis and enzyme activity measurement

The POCKET program (http://biogeometry.duke.edu/software/proshape) revealed the presence of only two identical pockets, one at each end of the antiparallel local two-fold related CD–CD pair, of size sufficient to accommodate the pteridin ring of a substrate. To prove that the pocket represents the CD active site, we carried out site-directed mutagenesis of some invariant residues associated with the pocket (Figure 6A and B), including D412, D479, M373 and N501 (Figure 2).

Stratagene's Quickchange Site-directed Mutagenesis kit was used in the site-directed mutagenesis of FTCD. The desired mutations were confirmed by DNA sequencing. All mutant proteins, purified using a similar procedure described above, were identical in mass (about 0.5 million Dalton) to the wild-type protein.

The cyclodeaminase activity of FTCD was assayed in duplicate or triplicate using a published procedure (MacKenzie, 1980). The substrate is freshly prepared 5*N*-formimino-THF following the method described in the procedure. The specific activity of the native FTCD is 106.8 ± 2.7 ìmol/min/mg protein.

Crystal structure coordinates

Coordinates have been deposited with the Protein Data Bank (accession no. 1TT9).

Acknowledgements

We thank A Choudhary for technical assistance and the Structural Biology Center staff at Argonne National Laboratory, especially Dr S Ginell, for assistance in the diffraction data collection. The work was supported by grants from NIH and the Welch Foundation to WC and FAQ. FAQ is an HHMI Investigator.

References

Bashour A-M, Bloom GS (1998) 58K, a microtubule-binding Golgi protein, is a formiminotransferase cyclodeaminase. *J Biol Chem* **273:** 19612–19617

Beaudet R, Mackenzie RE (1976) Formiminotransferase cyclodeaminase from porcine liver. An octomeric enzyme containing bifunctional polypeptides. *Biochim Biophys Acta* **453:** 151–161

Brünger AT, Adams PD, Clore GM, DeLano WL, Gros P, Grosse-Kunstleve RW, Jiang JS, Kuszewski J, Nilges M, Pannu NS, Read RJ, Rice LM, Simonson T, Warren GL (1998) Crystallography & NMR system: a new software suite for macromolecular structure determination. *Acta Crystallogr D* **54:** 905–921

Collaborative Computational Project No. 4 (1994) The CPP4 suite: programs for protein crystallography. *Acta Crystallogr D* **50:** 760–763

Dubochet J (1988) Cryo-electron microscopy of vitrified specimens. *Q Rev Biophys* **21:** 129–228

Findlay WA, MacKenzie RE (1988) Renaturation of formiminotransferase-cyclodeaminase from guanidine hydrochloride. Quaternary structure requirements for the activities and polyglutamate specificity. *Biochemistry* **27:** 3404–3408

Finer-Moore JS, Maley GF, Maley F, Montfort WR, Stroud RM (1994) Crystal structure of tymidylate synthase from T4 phage: component of a deoxynucleoside triphosphate-synthesizing complex. *Biochemistry* **33:** 15459–15468

Gao Y, Sztul E (2001) A novel interaction of the Golgi complex with the vimentin intermediate filament cytoskeleton. *J Cell Biol* **152:** 877–894

Gao YS, Alvarez C, Nelson DS, Sztul E (1998) Molecular cloning, characterization, and dynamics of rat formiminotransferase cyclodeaminase, a Golgi-associated 58-kDa protein. *J Biol Chem* **273:** 33825–33834

Gao YS, Vrielink A, MacKenzie R, Sztul E (2002) A novel type of regulation of the vimentin intermediate filament cytoskeleton by a Golgi protein. *Eur J Cell Biol* **81:** 391–401

Huang X, Holden HM, Rauschel FM (2001) Channeling of substrates and intermediates in enzyme-catalyzed reactions. *Annu Rev Biochem* **70:** 149–180

Incaprera M, Rindi L, Bazzichi A, Garzelli C (1998) Potential role of the Epstein–Barr virus in systemic lupus erythematosus autoimmunity. *Clin Exp Rheumatol* **16:** 289–294

Jiang W, Baker ML, Ludtke SJ, Chiu W (2001) Bridging the information gap: computational tools for intermediate resolution structure interpretation. *J Mol Biol* **308:** 1033–1044

Johnson PJ, McFarlane IG (1993) Meeting report: International autoimmune hepatitis group. *Hepatology* **18:** 998–1005

Jones TA, Zou JY, Cowan SW, Kjeldgaard M (1991) Improved methods for building protein models in electron density maps and the location of errors in these models. *Acta Crystallogr A* **47:** 110–119

Kohls D, Sulea T, Purisima EO, MacKenzie RE, Vrielink A (2000) The crystal structure of the formiminotransferase domain of formiminotransferase-cyclodeaminase: implications for substrate channeling in a bifunctional enzyme. *Structure* **8:** 35–46

La Fortelle Ed, Bricogne G (1997) SHARP program for statistical heavy-atom refinement. *Methods Enzymol* **276:** 472–494

Lapierre P, Hajoui O, Homberg JC, Alvarez F (1999) Formiminotransferase cyclodeaminase is an organ-specific autoantigen recognized by sera of patients with autoimmune hepatitis. *Gastroenterology* **116:** 643–649

Lapierre P, Johane C, Alvarez F (2003) Characterization of the B cell response of patients with anti-liver cytosol autoantibodies in type 2 autoimmune hepatitis. *Eur J Immunol* **33:** 1869–1878

Lu G (1999) FINDNCS: a program to detect non-crystallographic symmetries in protein crystals from heavy atom sites. *J Appl Crystallogr* **32:** 365–368

Ludtke SJ, Jakana J, Song JL, Chuang DT, Chiu W (2001) A 11.5 Å single particle reconstruction of GroEL using EMAN. *J Mol Biol* **314:** 253–262

MacKenzie RE (1980) Formiminotransferase-cyclodeaminase: a bifunctional enzyme from porcine liver. *Methods Enzymol* **66:** 626–628

MacKenzie RE, Baugh CM (1980) Tetrahydropterolypolyglutamate derivatives as substrates of two multifunctional proteins with folate-dependent enzyme activities. *Biochim Biophys Acta* **611:** 187–195

Murley LL, MacKenzie RE (1995) The two monofunctional domains of octameric formiminotransferase-cyclodeaminase exist as dimers. *Biochemistry* **34:** 10358–10364

Murley LL, MacKenzie RE (1997) Monofunctional domains of formiminotransferase-cyclodeaminase retain similar conformational stabilities outside the bifunctional octamer. *Biochim Biophys Acta* **1338:** 223–232

Otwinowski Z, Minor W (1997) Processing of X-ray diffraction data collected in oscillation mode. *Methods Enzymol* **276:** 307–326

Rosenblatt D (1995) Inherited disorders of folate transport and metabolism. In *The Metabolic and Molecular Bases of Inherited Diseases*, Scriver CR, Beaudet AL, Sly WS, Valle D (eds) pp 3111–3128. New York: McGraw-Hill

Shane B, Stokstad ELR (1984) Folates in the synthesis and catabolism of histidine. In *Folates and Pterins*, Blakley RI, Benkovic SJ (eds) Vol. 1, pp 433–455. New York: Wiley

Solans A, Estivill X, de la Luna S (2000) Cloning and characterization of human FTCD on 21q22.3, a candidate gene for glutamate formiminotransferase deficiency. *Cytogenet Cell Genet* **88:** 43–49

Weeks CM, Hauptman HA, Smith GD, Blessing RH, Teeter MM, Miller R (1995) Crambin: a direct solution for a 400-atom structure. *Acta Crystallogr D* **51:** 33–38